Journal of Hydrology 608 (2022) 127661

Contents lists available at ScienceDirect

Journal of Hydrology

journal homepage: www.elsevier.com/locate/jhydrol

Research papers

Simple approximate closed-form expressions for tracer injection in aquifer with a radially converging or diverging flow field

Dominique Thiéry

BRGM, 3 Avenue Claude Guillemin, BP 36009, F-45060 Orléans Cedex 2, France

ARTICLE INFO

"This manuscript was handled by Corrado Corradini, Editor-in-Chief, with the assistance of Patrick Lachassagne, Associate Editor"

Keywords:
Radial flow tracer tests
Closed-form approximation
Dimensional expression
Field test applications

ABSTRACT

The exact solution for the concentration breakthrough curves resulting from a solute injection in radially converging flow in an aquifer obtained using Laplace transforms has a complex form difficult to compute, and cannot be given in closed-form expression. This makes it difficult to use for tracer tests analysis in radial flow. To overcome this difficulty new simple approximate but accurate closed-form expressions are derived in the present paper for slug and continuous injections. The improvement of accuracy of these new closed-form expressions is demonstrated. The paper establishes also that the breakthrough curves resulting from slug injections into a radially diverging or radially converging flow are exactly identical at the sampling well in domains having the same spatial extension. Solutions were also derived for tracers or solutes subject to degradation.

The new closed-form expressions were used for the analysis of 12 field tracer tests to highlight the difference in transport parameters determination compared to previous approximate expressions.

Nomenclature

Notation	Definition	Unit	Relation
A	Intermediate variable	$[L^2T^{-1}]$	$A = Q/2\pi h\omega$
C	Concentration	$[ML^{-3}]$	
C_D	Dimensionless concentration	[-]	$C_D = C/C_{ref}$ or C/C_0
C_{ref}	Reference concentration	$[ML^{-3}]$	$C_{ref} = M/(\pi r_L^2 h\omega)$
C_0	Injected concentration	$[ML^{-3}]$	$C_0 = q_m/Q$
D_L	Longitudinal dispersion coefficient	$[L^2T^{-1}]$	$D_L = \alpha_L\lvert u\rvert$
erfc()	Complementary error function	[-]	
F	Slug injection: F=0; continuous injection: F=1	[-]	
f_P	Correcting factors for Péclet number	[-]	
f_T	Correcting factors for dimensionless time	[-]	
h	Aquifer thickness	[L]	
K	Normalization constant	[-]	
M	Injected mass	[M]	
P	Péclet number	[-]	$P = r_L/\alpha_L$
Q	Injected or pumped flow rate	$[L^3T^{-1}]$	
q_m	Mass flux	$[MT^{-1}]$	
R	Retardation coefficient	[-]	
r	Radial distance	[L]	
r_D	Dimensionless radial distance	[-]	$r_D = r/r_L$
r_L	Radial distance to outer well	[L]	
t	Time	[T]	
t_a	Advection time from outer to center	[T]	$t_a = \pi r_L^2 h\omega/Q$
t_D	Dimensionless time	[-]	$t_D = t/t_a$
T_g	First-order decay time constant	[T]	$T_g = 1/\lambda$
T_{gD}	Dimensionless decay time constant	[-]	$T_{gD} = T_g/t_a$
u	Pore velocity	$[LT^{-1}]$	
α_L	Longitudinal dispersivity	[L]	
α_T	Transverse dispersivity	[L]	
ε	Diverging flow: +1; converging flow: -1	[-]	
θ	Angular coordinate	[-]	
λ	First-order decay constant	$[T^{-1}]$	
ω	Kinematic porosity	[-]	

(*continued on next column*)

(*continued*)

1. Introduction

Tracer tests are widely used to determine non-reactive parameters governing transport in porous media, such as the effective porosity, the retardation factor and the dispersivities. Tracer tests may be performed from an injection well to a pumping well. If the flow rates in the wells are small, the flow is nearly 1D Cartesian and represents the background flow under natural conditions in the aquifer. There are then simple exact expressions to describe the time evolution of the concentration at the pumping well corresponding to an instantaneous injection of tracer (slug injection) or to a constant rate mass flux injection (continuous injection). Analyzing the monitored breakthrough curve (BTC) with a software such as CXTFIT (Toride et al., 1999), TRACI95 (Käss, 1998), QTRACER2 (Field, 2002), TRAC (Gutierrez et al., 2013) using these 1D expressions enables to determine the transport parameters. Tracer tests

https://doi.org/10.1016/j.jhydrol.2022.127661
Received 17 October 2021; Received in revised form 26 January 2022; Accepted 21 February 2022
Available online 28 February 2022

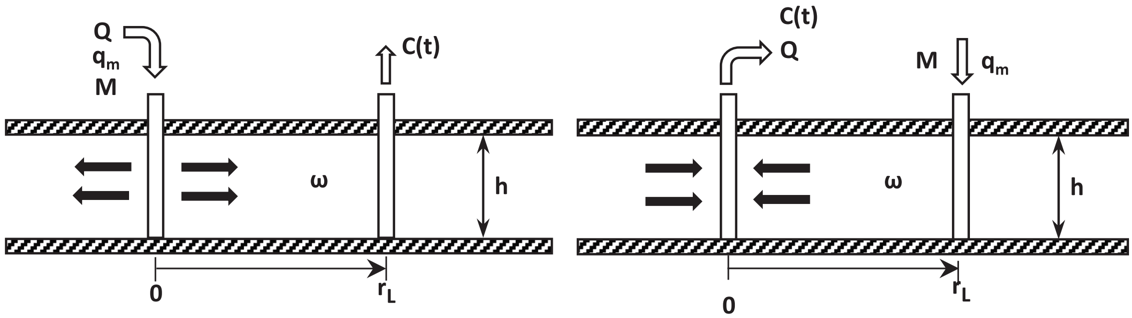

Fig. 1. Schematic diagram of radially diverging (left) or converging (right) tracer test. (Q is pumped or injected flow rate, q_m is injected mass flux, M is injected mass, h is aquifer thickness, ω is kinematic porosity, r_L is radial distance from center well to outer well, C(t) is concentration as a function of time).

under natural conditions are however difficult to manage, because of difficulty in determining the exact direction of flow, and the long duration of the tests resulting from the generally low velocities. Tracer tests in radially converging flow are widely used to overcome these difficulties, and tests in radially diverging flows can also be used for some applications (Fig. 1).

In both cases there are two wells: the first well located at the center of the radial flow, and the second well located laterally at the radial distance r_L from the center, called the outer well. In a diverging flow: the central well is an injection well where the tracer is introduced, and the sampling well is located at the distance r_L. In a converging flow, it is the opposite: the tracer is introduced in the outer well, and the central well is a pumping well where the tracer is sampled. The domain extension may be of two types: a semi-infinite domain extending from the central well to infinity, referred in this paper as an "unbounded domain", or a bounded domain extending only from the central well to the outer well. An unbounded domain would seem a priori to be closer to the field reality, but as will be discussed later, the solution of the convection–dispersion equation in converging flow generates a non-physical upstream dispersion that is reduced when considering a bounded domain.

Interpretation of tracer tests in radial flow is difficult because there are no exact closed-form solutions available for diverging flows, and the solutions available for converging flow, using Laplace transform or Airy functions are difficult to include in an interpretation software.

The purpose of this paper is to establish easy to use approximate closed-form expressions describing the evolution of the concentration of a tracer or solute in a radially converging or diverging flow field in bounded or unbounded domain. Closed-form expressions will be also established for solutes subject to degradation.

2. Previous work

Numerous papers addressed with different approaches the solution of radial flow tracer tests in diverging or converging flow, in bounded or unbounded domain.

2.1. Solutions for diverging flow only:

Ogata (1958) presented the exact solution for a continuous injection in diverging flow but its expression requires the integration of a rational fraction of Bessel functions of the first and second kind, hence the numerical calculation of this function is very complex.

2.2. Solutions for converging and diverging flow:

Sauty (1980) used a numerical finite differences model to compute the BTCs, and presented approximations by analytical functions and type curves for the concentration normalized by the maximum concentration C/C_{max}. However the results, which do not compare well to exact solutions, are only for Péclet numbers greater than 5 or 10, depending on the selected function, and for a slug injection refer only to the C/C_{max} ratio. Welty and Gelhar (1994) gave an approximate solution for high Péclet numbers. Wang and Crampon (1995) used a numerical model, with an outer boundary located far from the outer well, to fit analytical functions after applying correction factors to them. Their results which use a great number of correcting factors are approximate, as will be seen, apply only to Péclet numbers greater than 3, and also refer only to the C/C_{max} ratio.

2.3. Solutions for converging flow only:

Moench (1989), using Laplace transform, presented the exact closed-form analytical solution for converging flow in a bounded domain, i.e. without dispersion upstream of the injection well, as pointed out by Zlotnik and Logan (1996). Moench (1995) gave solutions for converging flow with double porosity. Chen et al. (1996) presented the exact solution for converging flow in an unbounded domain. Their analytical solution, involving Airy functions of complex arguments and Laplace inversion, are however quite difficult to compute due to the numerical back-transformation of the solutions in the Laplace domain to the time domain. Becker and Charbeneau (2000) presented also a solution for converging flow using Airy functions and Laplace transform. Chen et al. (2002) presented a new exact solution in bounded domain somewhat simpler, with Laplace transform but without Airy functions. Chen et al. (2003a) analyzed the effect of the well bore mixing volume. Chen et al. (2003b) derived semi-analytical solutions with a scale-dependent dispersivity.

2.4. Special configurations:

Wang and Zhan (2013) developed semi-analytical solutions of radial reactive solute transport in an aquifer–aquitard system in diverging flow, via Laplace transform and finite Fourier transform techniques and numerical inversion. Csanady (1973), Pérez Guerrero and Skaggs, (2010), Natarajan, (2016) proposed various schemes where the longitudinal dispersivity is not constant but increases with transport distance. Irvine et al. (2020) described a method to reduce unwanted upstream dispersion in 2D discretized numerical models. Akanji and Falade (2018) derived a solution to the radial transport of tracer under the influence of linear drift. Their solution, which uses Tricomi-Kummer functions and requires a numerical Laplace inversion, shows that the effect of the drift becomes progressively more pronounced at later times. Van Genuchten (1981, 1985) presented solutions, in Cartesian coordinate system, for solutes involved in sequential first-order decay reactions.

3. Mathematical formulation

A homogeneous and isotropic aquifer, of infinite horizontal extent and constant thickness *h* and effective porosity *ω* is considered. A well of negligible radius, located in this aquifer with a constant injection or pumping rate, creates a steady-state diverging or converging radial flow field. Tracer transport in the aquifer occurs by radial advection and by mechanical dispersion. The effects of molecular diffusion and also the effects of both extraction and injection well mixing volumes are considered as negligible. Tracer degradation is not considered in this section, however closed-form expressions including degradation will be presented in Section 7.5.

Two mass injection regimes are studied: a slug (or Dirac) injection where a mass *M* of tracer is injected instantaneously, or a continuous injection where a constant mass flux q_m is injected. The continuous injection corresponds to the integration over time of slug injections.

3.1. Diverging flow

The well injects a constant positive flow rate *Q*. At the initial time a mass *M* of tracer, or a constant mass flux q_m of tracer, is injected instantaneously into the well. The concentration is monitored in a sampling well situated at a distance r_L. The system is perfectly axisymmetric and the mass transport equation (Sauty, 1980) is

$$R\frac{\partial C}{\partial t} = D_L\frac{\partial^2 C}{\partial r^2} - u\frac{\partial C}{\partial r} \tag{1}$$

Where *r* is the radial distance from the well, *t* is the time from the start of the tracer injection, *C* is the tracer concentration, *u* is the pore velocity, D_L is the longitudinal dispersion coefficient, and *R* is the tracer retardation factor resulting from a partition coefficient k_d between the liquid phase and a solid phase. The geometry being axisymmetric the transverse dispersion coefficient has no influence and doesn't appear in the equation. Assuming that $D_L = \alpha_L \cdot |u|$, neglecting the molecular diffusion, and expressing the velocity as $u = Q / 2\pi r h\omega = A / r$, where $A = Q / 2\pi h\omega$, into eq. (1) results in:

$$R\frac{\partial C}{\partial t} = \alpha_L\frac{A}{r}\frac{\partial^2 C}{\partial r^2} - \frac{A}{r}\frac{\partial C}{\partial r} \tag{2}$$

3.2. Converging flow

The well is pumped at a constant positive flow rate *Q*. At the initial time a mass *M* of tracer, or a constant mass flux q_m of tracer, is injected in a nearby borehole at a distance r_L, without disturbing the flow field in the aquifer. The concentration is monitored in the pumped well. The system is not axisymmetric and the mass transport equation (Sauty, 1980) is

$$R\frac{\partial C}{\partial t} = \alpha_L|u|\frac{\partial^2 C}{\partial r^2} + \frac{\alpha_T|u|}{r^2}\frac{\partial^2 C}{\partial \theta^2} - u\frac{\partial C}{\partial r} \tag{3}$$

where α_T is the transverse dispersivity, θ the angular coordinate, and $u = -A / r$ is negative.

Because the concentration in the pumped well is the average over the negligible well radius, Sauty (1977a, 1980) shows that it is possible to consider the average concentration at a radius *r*.

$$C(r,t) = \frac{1}{2\pi}\int_0^{2\pi} C(r,\theta,t)\cdot d\theta \tag{4}$$

Applying this transformation to eq. (3), the second term depending on θ and α_T disappears. The average concentration does not depend any more on the transverse dispersivity and eq. (5), similar to eq. (2) for diverging flow, is obtained, with only a change of sign in the last term.

$$R\frac{\partial C}{\partial t} = \alpha_L\frac{A}{r}\frac{\partial^2 C}{\partial r^2} + \frac{A}{r}\frac{\partial C}{\partial r} \tag{5}$$

3.3. Equation for both diverging and converging flow

The equations for diverging and converging flow may be combined as:

$$R\frac{\partial C}{\partial t} = \alpha_L\frac{A}{r}\frac{\partial^2 C}{\partial r^2} - \varepsilon\frac{A}{r}\frac{\partial C}{\partial r} \tag{6}$$

where $\varepsilon = +1$ for diverging flow and $\varepsilon = -1$ for converging flow.

To obtain a dimensionless equation let the following variables:

$t_a = \pi r_L^2 h\omega/Q = r_L^2/2A$ = advection time from the injection point to the observation point located at distance r_L.

$C_{ref} = M/(\pi r_L^2 h\omega)$ = Injected mass divided by the water volume within the distance r_L, for a slug injection.

$C_0 = q_m/Q$ = Equivalent injected concentration, for a continuous mass flux injection.

$P = r_L/\alpha_L$ = Péclet number.

Using the dimensionless variables: $r_D = r/r_L$; $t_D = t/t_a$; $C_D = C/C_{ref}$, or $C_D = C/C_0$, the mass transport equation eq. (6), for diverging or converging flow becomes

$$2R\frac{\partial C_D}{\partial t_D} = \frac{1}{P\cdot r_D}\frac{\partial^2 C_D}{\partial r_D^2} - \varepsilon\frac{1}{r_D}\frac{\partial C_D}{\partial r_D} \tag{7}$$

where $\varepsilon = +1$ for diverging flow and $\varepsilon = -1$ for converging flow. The only parameter of this eq. (7) is the Péclet number *P*, not mentioning the retardation factor *R* which can be included in t_D

Transport boundary conditions

The transport boundary condition at the central well ($r_D = 0$) is

$$C_D - \frac{1}{P}\frac{\partial C_D}{\partial r_D} = F \quad \text{in diverging flow} \tag{8a}$$

$$\frac{\partial C_D}{\partial r_D} = 0 \quad \text{in converging flow} \tag{8b}$$

with $F = 0$ for a slug injection and $F = 1$ for a continuous injection.

In an unbounded domain, the outer boundary condition ($r_D=\infty$) is

$$\frac{\partial C_D}{\partial r_D} = 0 \quad \text{or} \quad C_D = 0 \tag{8c}$$

In a bounded domain, the outer boundary condition ($r_D = 1$) is

$$\frac{\partial C_D}{\partial r_D} = 0 \quad \text{in diverging flow} \tag{8d}$$

$$C_D + \frac{1}{P}\frac{\partial C_D}{\partial r_D} = F \quad \text{in converging flow} \tag{8e}$$

4. Unbounded domain versus bounded domain

The dispersion term in eq. (6) is a Fickian diffusion process which generates dispersion in all directions, downstream but also upstream. In a converging flow the upstream dispersion generates mass transport upstream of the injection well, which is non-physical because mechanical dispersion is due to the heterogeneity of the velocity field caused by the heterogeneity of the medium. However the velocity field heterogeneity cannot lead to counter flow velocity. In fact, the upstream dispersion is essentially due to the assumption that dispersion D_L is equal to $\alpha_L \cdot |u|$, with α_L independent of distance. Yet it has been observed that the average value of α_L between two points is clearly increasing with their distance (Sauty, 1980, Pérez Guerrero and Skaggs, 2010, Chen et al. 2003b, Natarajan, 2016).

A method to reduce or cancel the upstream dispersion is to assume, according to Csanady (1973) and Chen et al. (2003b), that the longitudinal dispersivity is not constant but increases with transport distance, thus with travel time, from a small or nil initial value to a large final value. However, this method requires the dispersivity-distance relationship which is seldom available. Irvine et al. (2020) describe a method to reduce unwanted upstream dispersion in 2D discretized numerical models by setting a lower dispersivity in areas upstream of the injection wells.

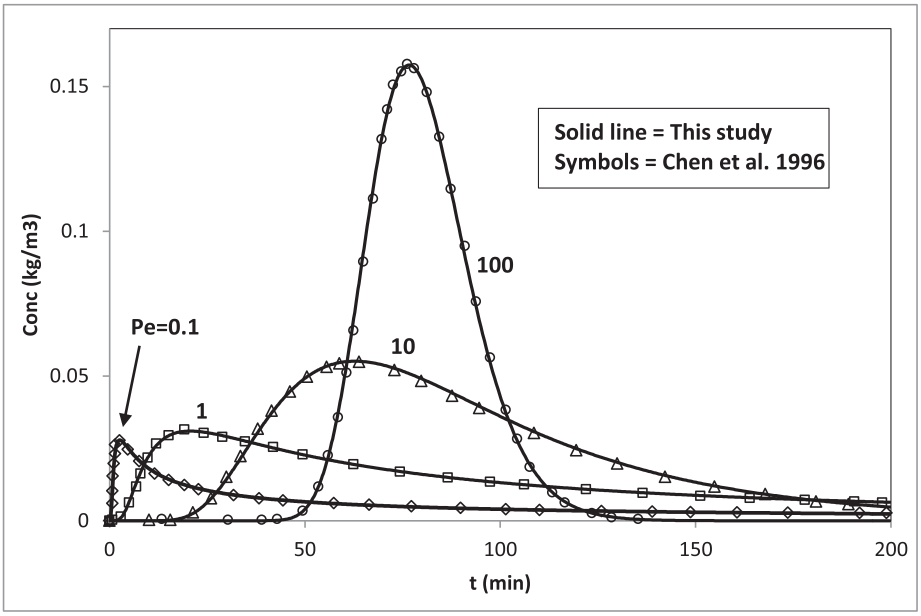

Fig. 2. Comparison of dimensional BTCs obtained with the numerical model to the Chen et al. (1996) solution, in a hypothetical condition in converging flow in unbounded domain.

Another classic, however somewhat artificial, way to reduce the upstream dispersion is to limit the modeled domain to the outer injection well which corresponds to a bounded domain. In fact, this cancels the dispersivity upstream of the injection well, but not all the upstream dispersion that results from the symmetric dispersion term in eq. (5).

To deal with this issue of bounded or unbounded domain, it has been decided in this paper, for the sake of completeness, to establish closed form expressions for both the unbounded and the bounded domain. A comparison of the transport parameters obtained in a tracer test analysis using expressions for a bounded or unbounded domain will be presented in Appendix C. Although the bounded domain applies only to converging flow, the closed-form expressions have also been established in diverging flow for comparison, and for possible use in particular configurations.

5. Method for obtaining approximate closed-form expressions

To obtain closed-form expressions easy to use and to integrate into a computer code, without Airy functions or Laplace inversion, which is the main goal of this paper, an approach somewhat similar to that of Wang and Crampon (1995) was used. Starting from simple approximate closed-form expressions for a slug injection or a continuous injection in 1D Cartesian coordinate, two correction coefficients, applied to the Péclet number P and the dimensionless time t_D, were introduced into the expression to obtain a simple expressions that most accurately reproduce the exact solutions.

Since the exact solutions, that involve Airy functions or Laplace inversions, were difficult to determine, another method was used to calculate them. A finite volume groundwater flow and transport numerical model was used to obtain numerically exact BTCs resulting from slug or continuous injections for a wide range of Péclet numbers, from 0.1 to 1000, that will be used later to determine the simple approximate closed-form expressions. The accuracy of the model simulations was checked by comparing them to the available exact solutions of a limited number of BTCs in converging flow, as presented in figures from the literature, mainly in Moench (1989), Chen et al. (1996, 2002). The numerical model was also used to generate the exact solutions in diverging flow that are not available in the literature, and to take into account the tracer degradation as will be shown in Section 7.5.

6. Numerical solutions in converging and diverging flow

The numerical calculations were performed with MARTHE code (Thiéry, 2010, 2015b; Vanderborght et al., 2005; Thiéry and Picot-Colbeaux, 2020). In the numerical code, the mass transport equation is solved numerically using a total-variation-diminishing (TVD) method implemented with a flux limiter (Leonard, 1988), which produces very little numerical dispersion. Due to the axisymmetric geometry the calculations were performed with a 1D radial grid. Following Sauty (1977a), a non-uniform spatial discretization was implemented to ensure a constant numerical Courant number. As the pore velocity decreases with the distance from the central well, the grid size also decreases with distance. Four sets of BTCs were generated with the model: in converging flow and in diverging flow, and both of them in bounded or unbounded domain.

6.1. Discretization, outer boundary condition and initial conditions

In the model a fine 1D radial grid is used and the steady-state radial flow field is computed first. To obtain the radial flow field a source term, injection or pumping, is set in the cell located at the origin of the grid, and a constant hydraulic head is prescribed, a Dirichlet condition, in the model outer limit located very far from the wells. This prescribed hydraulic head automatically generates the desired radial flow. Mass transport is then computed in transient state starting from an initial concentration equal to zero in the whole domain.

For an unbounded domain the outer boundary for transport was located far enough away from the central well to have no influence, usually at a dimensionless radial distance r_D equal to 3. For Péclet numbers as low as 0.1, or for continuous injections, the transport outer boundary was located farther, at a dimensionless radial distance equal to 7. The concentration was prescribed at this outer boundary, but it was verified that this boundary being located far enough away, the results obtained with a no-flow boundary were identical. For a bounded domain the grid extension, hence the outer boundary for transport, was limited to the outer well, i.e. at a dimensionless distance r_D equal to 1. At this outer boundary, a constant hydraulic head is prescribed, as was done for the unbounded domain to generate the desired radial flow, and a no-flow boundary condition was set for the mass transport, without prescribing the concentration. However exactly the same results were

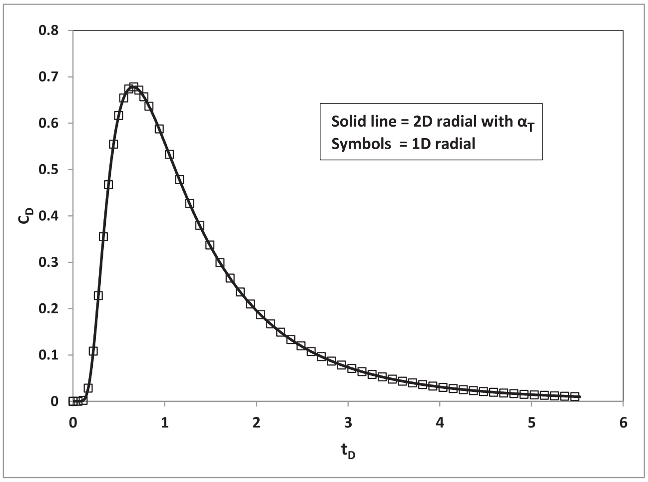

Fig. 3. 2D numerical simulation with transverse dispersivity in converging flow: comparison with a 1D radial simulation. (Péclet number = 5, transverse dispersivity = 0.2 × α_L).

obtained keeping the former quasi-infinite grid and setting a nil dispersivity in all cells located at a dimensionless distance larger than 1. The dimensionless radial distance r_D equal to 3, or equal to 7, was discretized in 3000 cells and the dimensionless time t_D up to 5 was divided in 10,500 time steps.

6.2. *Verification of the numerical scheme and discretization in converging flow*

The 1D radial numerical scheme and discretization was checked by comparison with available solutions in converging flow in unbounded and bounded domains.

A first verification was done in unbounded domain for Péclet numbers ranging from 0.1 to 300. Fig. 2 illustrates that, even for Péclet numbers as small as 0.1, the numerical solutions are identical to Chen et al. (1996) analytical solution as depicted in their Fig. 2.

A second verification was done in bounded domain by comparison to Moench (1989) and to Chen et al. (2002) analytical solution for Péclet numbers ranging from 0.1 to 200. It is shown in Appendix A that the numerical solutions are also identical to the exact analytical solution (Figs. A1 and A2).

It was also verified numerically that, as demonstrated by Sauty (1977a, 1980), the transverse dispersion has no influence. A simulation was performed, with the same numerical code, in 2D radial coordinates in an unbounded domain, for a Péclet number equal to 5 with a transverse dispersivity equal to 0.2 × α_L. Fig. 3 confirms that the simulated average concentration along the production well radius is identical to the concentration obtained with a 1D simulation without transverse dispersivity which is a further verification of the numerical code accuracy. The accuracy of the solutions obtained with the numerical model having been carefully verified, these numerical solutions will be called "exact solutions" from here on in the paper.

6.3. *Numerical solution for a slug injection or a continuous injection in a diverging flow in unbounded domain*

The exact solutions for diverging flow being not available in the literature, they are also generated with the numerical model. The accuracy of the numerical modeling being verified in converging flow, it is assumed that the numerical scheme and the spatial and time discretization can also be used for diverging flow using a different boundary condition. For this calculation the outer boundary is set at a distance sufficient to obtain there a negligible concentration, less than 1/1000 of maximum concentration. Because the flow field is axisymmetric, the transverse dispersivity having no influence is not included in the calculation. Fig. 4 compares the BTCs resulting from a slug injection in diverging flow and in converging flow in an unbounded domain for Péclet numbers ranging from 0.1 to 100. It appears, though it has not been demonstrated, that the BTCs are absolutely identical. Fig. 5 compares the concentrations profiles at t_D = 0.25 & t_D = 0.5 for a slug injection in diverging flow and in converging flow in an unbounded domain, for a Péclet number equal to 3: although the profiles are essentially different, the concentrations at the sampling well are identical. This result is quite different from the results obtained by Wang and Crampon (1995), who used the same outer boundary condition, probably because the radial extent of their grid was too small, especially for small Péclet numbers.

Since the continuous injection corresponds to the integration over time of slug injections, the computed BTCs in converging and in

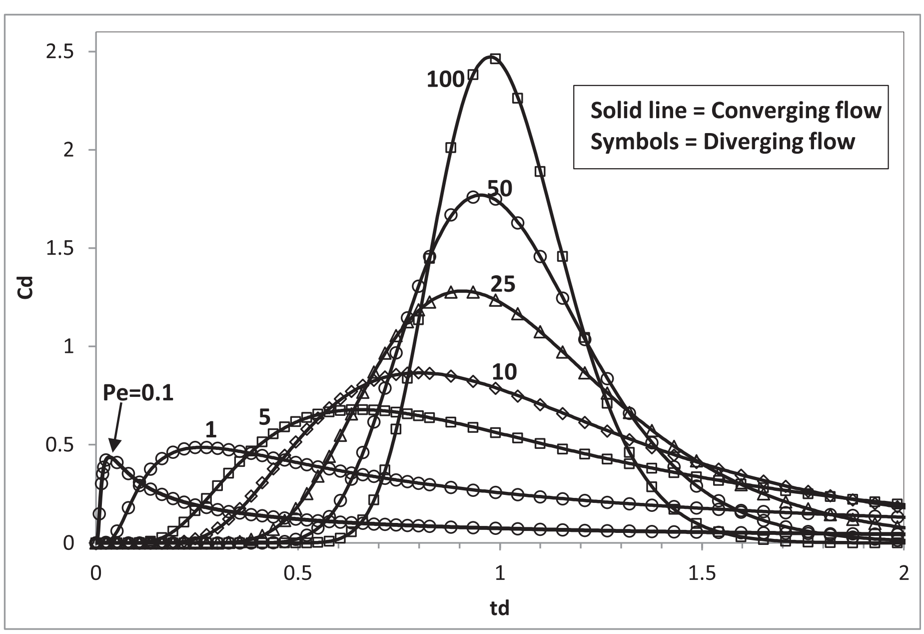

Fig. 4. Comparison of the numerical solution for a slug injection in unbounded domain in converging flow and in diverging flow in dimensionless coordinates.

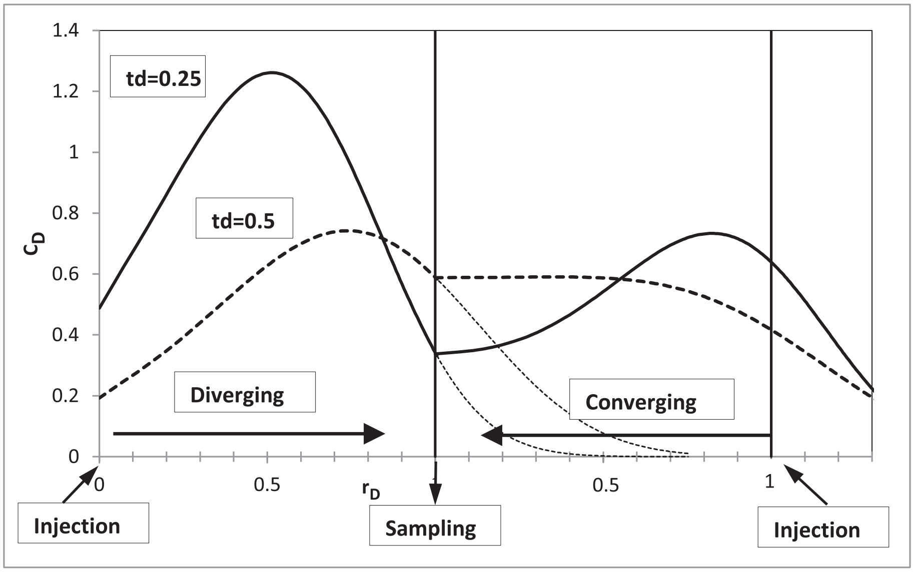

Fig. 5. Comparison of the numerical simulation of a slug injection in unbounded domain in converging flow and in diverging flow for a Péclet number equal to 3; t_D = 0.25 & t_D = 0.5. Left: diverging flow; right converging flow.

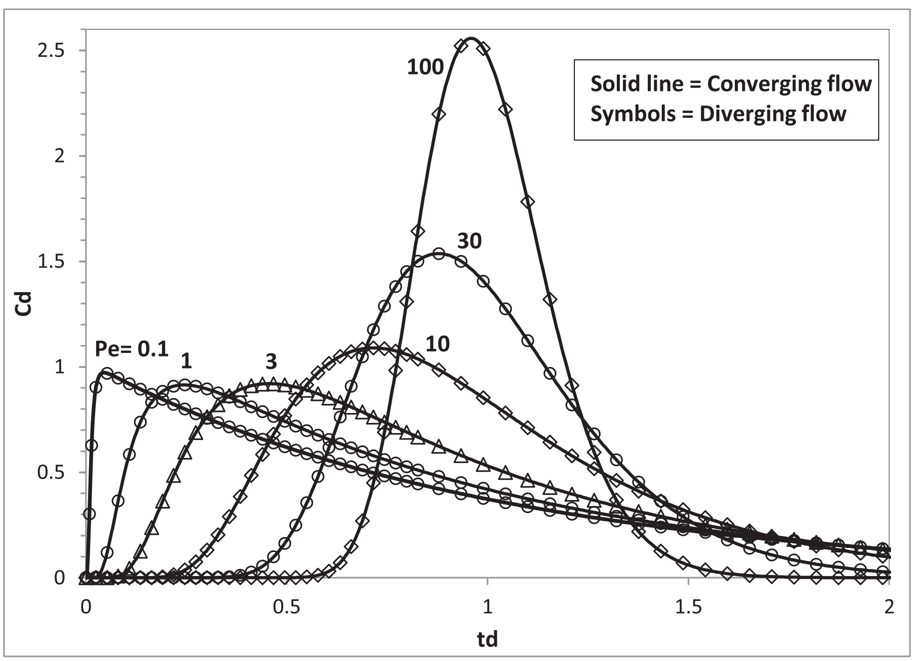

Fig. 6. Comparison of the numerical solution for a slug injection in bounded domain in converging and in diverging flow in dimensionless coordinates.

diverging flow should also be identical, which was verified by our simulations. The numerical solution for BTCs from continuous injection in diverging flow, not displayed in the paper, are exactly identical to the corresponding BTCs in converging flow.

6.4. Numerical solution for a slug injection or a continuous injection in bounded domain

The BTCs resulting from a slug injection in bounded domain in diverging and in converging flow have been computed for Péclet numbers ranging from 0.1 to 200. Fig. 6 compares the BTCs obtained in diverging flow and in converging flow in a bounded domain. Similar to what was obtained in unbounded domain, it appears, though it has not been demonstrated, that in bounded domain also the BTCs are absolutely identical in diverging and in converging flow. Fig. 7 displays the concentrations profiles at $t_D = 0.25$ & $t_D = 0.4$ for a slug injection in diverging flow and in converging flow in bounded domain, for a Péclet number equal to 3. It illustrates that, as in unbounded domain, although the profiles are different, the concentrations at the sampling well are identical.

7. Approximate closed-form expressions

As explained in Section 5, the exact solutions needed to obtain the approximate closed-form expressions were obtained by numerical modeling. The exact solutions for slug injections and continuous injections were successively computed with the numerical model for 20 values of Péclet numbers ranging from 1 to 1000, or from 0.8 to 1000,

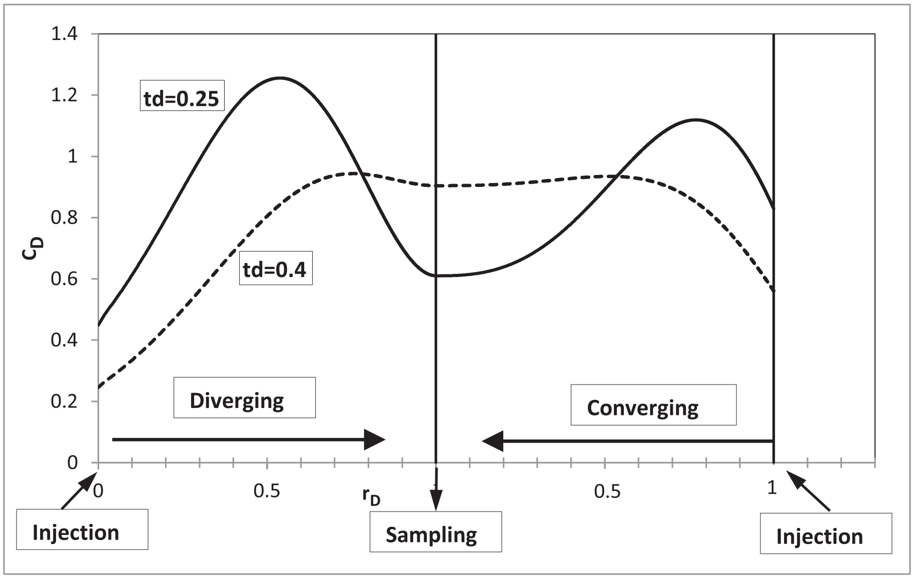

Fig. 7. Comparison of the numerical simulation of a slug injection in bounded domain in converging flow and in diverging flow for a Péclet number equal to 3; $t_D = 0.25$ & $t_D = 0.4$. Left: diverging flow; right converging flow.

for dimensionless time t_D ranging from 0 to 6. The solutions were calculated only in converging flow, as it has been shown that they were identical in diverging flow. For each solution, slug injection or continuous injection, a simple closed-form expression approximation F of the exact solution in the form of eq. (9) is selected

$$C_D(t_D) = F(P, t_D) \tag{9}$$

As in Wang and Crampon (1995) approach, two correction factors were introduced: a correction factor f_T on the dimensionless time and a correction factor f_P on the Péclet number to obtain a simple closed-form expression that most accurately reproduces the exact solutions. The following formulation for these correction factors, depending only of the Péclet number, was chosen

$$f_T = a + b{\cdot}P^c \text{ and } f_P = d + e{\cdot}P^f \tag{10}$$

In the equations the dimensionless time t_D is multiplied by f_T, and the Péclet number P is divided by f_P. The reason why P is divided by f_P, rather than multiplied by f_P, is that f_P was introduced as a multiplying factor on the dispersivity, hence a dividing factor on the Péclet number.

Introducing the two correction factors of eq. (10) into eq. (9) it becomes:

$$C_D(t_D) = F(P/f_P, f_T{\cdot}t_D) \tag{11}$$

The unique set of 6 constants a, b, c, d, e, and f is determined by optimization, using the Rosenbrock (1960) algorithm, to simultaneously reproduce as accurately as possible with eq. (11) a large set of around 20 BTCs corresponding to 20 values of the Péclet number. The optimization process maximizes the average Nash criterion (Nash and Sutcliffe, 1970) of the 20 BTCs obtained by eq. (11) with respect to the corresponding exact solutions.

Approximate expressions are established both for an unbounded domain (Section 7.1) and for a bounded domain (Section 7.2). The improvement of the new closed-form expression, compared to available approximate expressions, is demonstrated in Section 7.3. The application of the expressions for a solute subject to interactions resulting in a retardation coefficient is described in Section 7.4. The adaption of the closed-form expressions to solutes or tracers subject to degradation is presented in Section 7.5. A comparison of the transport parameters obtained in a tracer test analysis using expressions for a bounded or unbounded domain is given in Appendix C. It highlights the large variations in dispersivity values, but also in porosity, obtained according to the choice of geometry.

7.1. Approximate closed-form expressions in unbounded domain

Closed-form expressions were derived in unbounded domain for a continuous injection and for a slug injection.

7.1.1. Approximate closed-form expression for a continuous injection in unbounded domain

Two 1D closed-form expressions were tried to determine which one would produce the best results. The first expression eq. (12) is the solution for a constant rate mass injection in Cartesian coordinate. It was derived by Sauty (1977a) by integration of the solution reported by Bear (1972) for a slug injection into an infinite column:

$$C(x,t) = \frac{q_m}{2Q}\left\{\operatorname{erfc}\left[\frac{(x-ut)}{\sqrt{4D_L t}}\right] - \exp\left(\frac{x}{\alpha_L}\right){\cdot}\operatorname{erfc}\left[\frac{(x+ut)}{\sqrt{4D_L t}}\right]\right\} \tag{12}$$

The second expression considered, eq. (13), is a simplification of eq. (12) obtained by dropping its second term:

$$C(x,t) = \frac{q_m}{2Q}\operatorname{erfc}\left[\frac{(x-ut)}{\sqrt{4D_L t}}\right] \tag{13}$$

The results obtained with this expression turned out to be significantly closer to the exact solution, especially for Péclet numbers smaller than 3

In radial flow, at a distance $r = r_L$, considering the "average" pore velocity u_a defined as

$u_a = \frac{r_L}{t_a} = \frac{Q}{\pi h \omega r_L}$; $D_L = \alpha_L.u_a$. The equivalent formulation of eq. (13) in radial coordinate in dimensionless form is

$$C_D(t_D) = 0.5{\cdot}\operatorname{erfc}\left[\sqrt{\frac{P}{4t_D}}(1-t_D)\right] \tag{14}$$

This formulation is only a crude approximation of the exact solution. Introducing the two correction factors f_T and f_P, eq. (14) becomes:

$$C_D = 0.5{\cdot}\operatorname{erfc}\left[\sqrt{\frac{P/f_P}{4f_T{\cdot}t_D}}(1-f_T{\cdot}t_D)\right] \tag{15}$$

As explained before, the optimal set of 6 constants a, b, c, d, e, and f is determined by optimization to simultaneously reproduce as accurately as possible with eq. (15) the 20 BTCs corresponding to 20 values of the

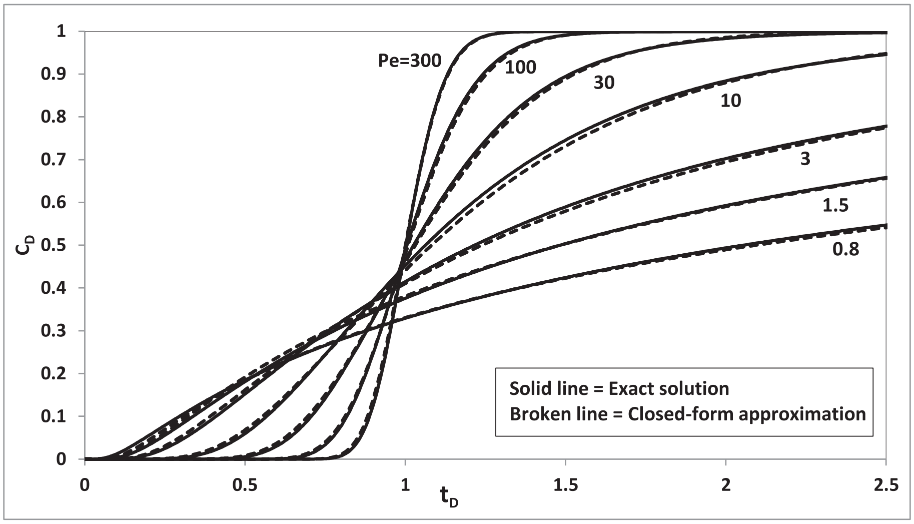

Fig. 8. Continuous injection in unbounded domain, converging flow and diverging flow.

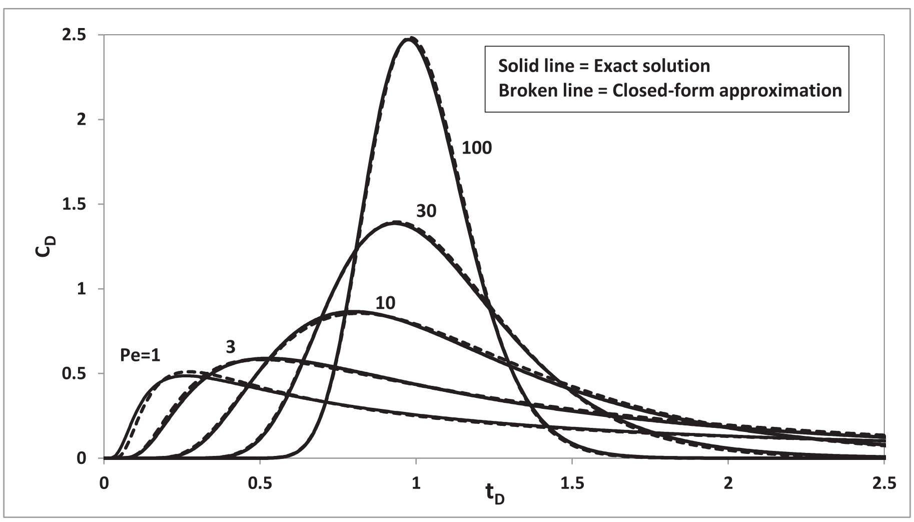

Fig. 9. Slug injection in unbounded domain in converging flow or diverging flow.

Péclet number. With this unique set of 6 constants a very good match was obtained for Péclet numbers ranging from 0.8 to 1000, and t_D ranging from 0 to 6 (See Fig. 8). The lowest Nash criterion of all curves is 0.9994.

The equations obtained for the correcting factors for a continuous injection in converging or diverging flow in unbounded domain are

$$f_T = 1.00627 - 0.44829 \cdot P^{-0.73712} \quad (16a)$$

$$f_P = 1.44488 - 0.21574 \cdot P^{-0.78005} \quad (16b)$$

7.1.2. Approximate closed-form expression for a slug injection in unbounded domain

Bear (1972) shows that the analytical solution for a slug injection into an infinite column is

$$C(x,t) = \frac{M}{\omega h w \sqrt{4\pi D_L t}} \cdot \exp\left[-\frac{(x-ut)^2}{4D_L t}\right] \quad (17)$$

where w is the width of the horizontal column.

In radial flow, at a distance $x = r_L$ and using u_a, the equivalent formulation in radial coordinate is

$$C(r_L,t) = \frac{M u_a}{Q\sqrt{4\pi\alpha_L u_a t}} \cdot \exp\left[-\frac{(r_L - u_a t)^2}{4\alpha_L u_a t}\right] \quad (18)$$

and in dimensionless variables

$$C_D(t_D) = \sqrt{\frac{P}{4\pi t_D}} \cdot \exp\left[-\frac{P}{4t_D}(1-t_D)^2\right] \quad (19)$$

However the derivative with respect to dimensionless time t_D of eq. (14), which gave a very good match for a continuous injection, is

$$C_D(t_D) = 0.5\sqrt{\frac{P}{4\pi t_D}} \cdot \frac{(t_D+1)}{t_D} \cdot \exp\left[-\frac{P}{4t_D}(1-t_D)^2\right] \quad (20)$$

Introducing the correction factors f_P. and f_T, eq. (20) becomes:

$$C_D(t_D) = 0.5 \cdot f_T \sqrt{\frac{P/f_P}{4\pi f_T \cdot t_D}} \cdot \frac{(f_T \cdot t_D + 1)}{f_T \cdot t_D} \cdot \exp\left[-\frac{P/f_P}{4 f_T \cdot t_D}(1 - f_T \cdot t_D)^2\right] \quad (21)$$

The leading factor f_T introduced into the first term is necessary to have an integral from $t_D = 0$ to ∞ equal to 1, i.e. to conserve mass.

As for the continuous injection, another unique set of 6 constants *a, b, c, d, e*, and *f* was determined by optimization to obtain the closest approximation of the 20 exact solutions for slug injections. Again a very

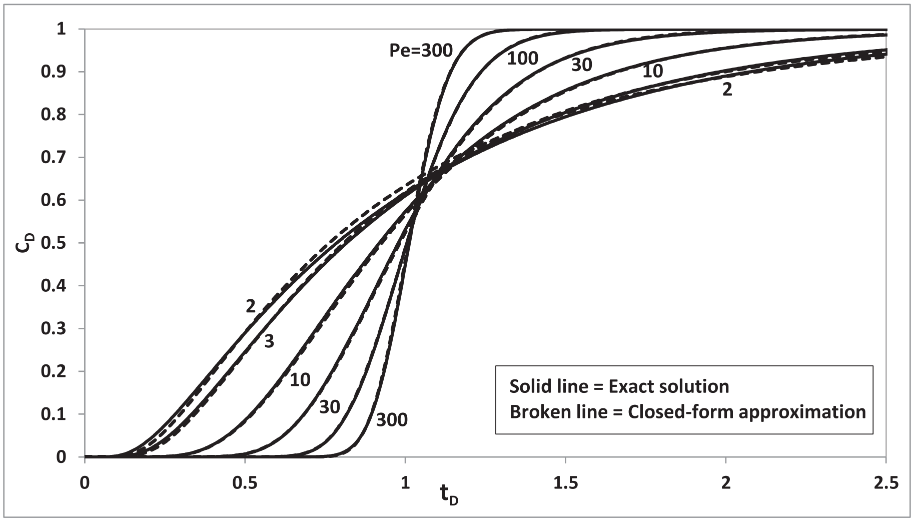

Fig. 10. Continuous injection in bounded domain, converging flow and diverging flow.

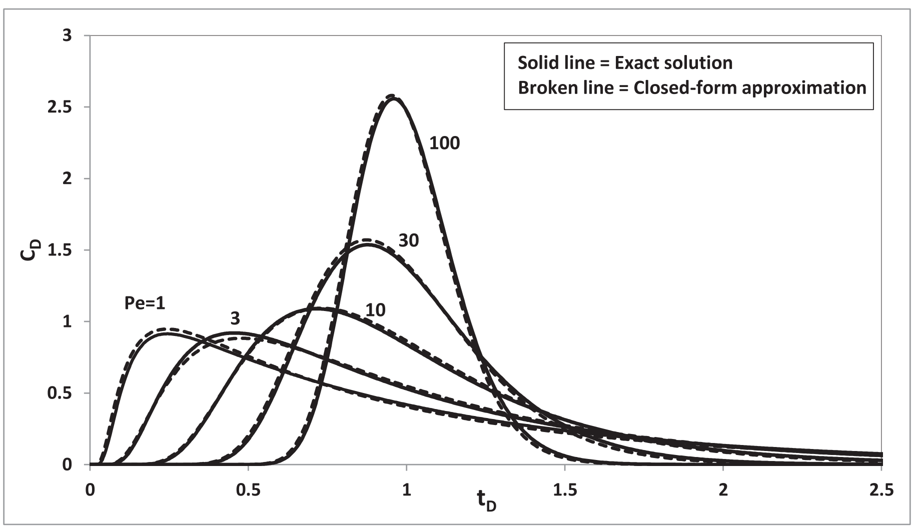

Fig. 11. Slug injection in bounded domain in converging flow or diverging flow.

good match is obtained for Péclet numbers ranging from 1 to 1000, and t_D ranging from 0 to 6 (See Fig. 9). The fit obtained with eq. (21) is significantly better than that obtained when fitting eq. (19) that could have seemed more natural. The lowest Nash criterion of all curves is 0.9922.

The equations obtained for the correcting factors for a slug injection in converging or diverging flow in unbounded domain are:

$$f_T = 1.00092 - 0.45272 \cdot P^{-0.87334} \tag{22a}$$

$$f_P = 1.51016 - 0.3189 \cdot P^{-0.09496} \tag{22b}$$

7.2. Approximate closed-form expressions in bounded domain

In the same manner as for an unbounded domain, closed-form expressions have been determined for a continuous injection and for a slug injection in bounded domain.

7.2.1. Approximate closed-form expression for a continuous injection in bounded domain

Among the 1D closed-form expressions that were tried, it is the solution for a step injection at fixed concentration in 1D Cartesian coordinate system that produces the best results. It is Ogata and Banks (1961) equation:

$$C_D(t_D) = 0.5\left\{\mathrm{erfc}\left[\sqrt{\frac{P}{4t_D}}(1 - t_D)\right] + \exp(P)\cdot\mathrm{erfc}\left[\sqrt{\frac{P}{4t_D}}(1 + t_D)\right]\right\} \tag{23}$$

This equation differs from equation (12) by a plus sign in front of the term exp().erfc() instead of a minus sign.

Introducing the correction factors f_P and f_T, eq. (23) becomes

$$C_D(t_D) = 0.5\left\{\mathrm{erfc}\left[\sqrt{\frac{P/f_P}{4f_T\cdot t_D}}(1 - f_T\cdot t_D)\right] + \exp(P/f_P)\cdot\mathrm{erfc}\left[\sqrt{\frac{P/f_P}{4f_T\cdot t_D}}(1 + f_T\cdot t_D)\right]\right\} \tag{24}$$

After determination of the optimal set of 6 constants *a, b, c, d, e*, and *f* a very good match is obtained for Péclet numbers ranging from 2 to 1000 (See Fig. 10). However, the fit is not quite as good for Péclet numbers lower than 2. The average Nash criterion for the 20 curves is 0.9998, and the lowest criterion is 0.9988.

The equations obtained for the correcting factors for a continuous injection in converging flow in bounded domain are

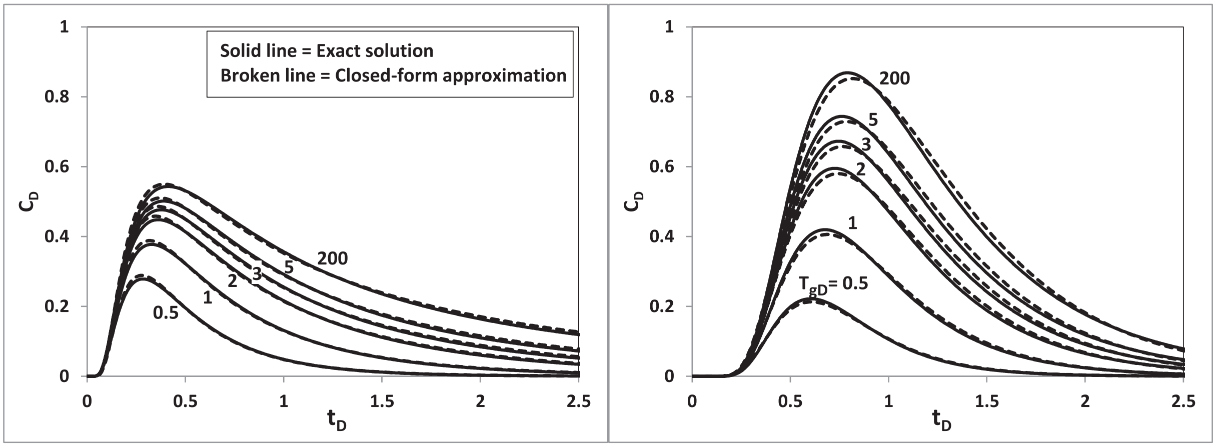

Fig. 12. Slug injection in converging flow or diverging flow in unbounded domain with various dimensionless decay time constants T_{gD}. Left: Péclet number = 2; Right: Péclet number = 10.

$$f_T = 1.17097 - 0.20663 \cdot P^{-1.87515} \quad (25a)$$

$$f_P = 1.43094 - 0.96565 \cdot P^{-0.47269} \quad (25b)$$

7.2.2. *Approximate closed-form expression for a slug injection in bounded domain*

Several classic closed-form expressions were tried. The derivative versus time of Ogata and Banks (1961) equation for a step injection in 1D Cartesian coordinate, Lenda and Zuber (1970), that was used by Sauty (1980):

$$C_D(t_D) = \sqrt{\frac{P}{4\pi}} \cdot t_D^{-3/2} \cdot \exp\left[-\frac{P}{4t_D}(1-t_D)^2\right] \quad (26)$$

did not result in a close match for all Péclet numbers after optimization of the set of 6 constants. The curves for low Péclet numbers were not modeled accurately. The selected closed-form expression is equation (18) for a slug injection in 1D Cartesian coordinate (Bear 1972). After determination of the optimal set of 6 constants *a, b, c, d, e*, and *f*, a very good match is obtained for Péclet numbers ranging from 1 to 1000 (See Fig. 11). For the sake of readability, the curves for Péclet numbers from 200 to 1000 do not appear in Fig. 11, but they are also very accurately reproduced. The average Nash criterion for the 20 curves is 0.9993, and the lowest Nash criterion is 0.9984.

$$C_D(t_D) = f_T \sqrt{\frac{P/f_P}{4\pi f_T \cdot t_D}} \cdot \exp\left[-\frac{P/f_P}{4f_T \cdot t_D}(1 - f_T \cdot t_D)^2\right] \quad (27)$$

The equations obtained for the correcting factors for a slug injection in converging flow in bounded domain are:

$$f_T = 0.99003 + 1.29039 \cdot P^{-0.72566} \quad (28a)$$

$$f_P = 1.51514 - 0.89053 \cdot P^{-0.29830} \quad (28b)$$

7.3. *Improvement of the new closed-form expressions compared to available expressions*

The improvement of the new closed-form expressions developed in the present paper has been demonstrated by comparison to two approximate closed-form available in radial flow: the closed-form described by Sauty (1980) for a slug injection in converging flow, and the closed-form described by Wang and Crampon (1995) for the whole BTC duration. The comparison is detailed in Appendix B. Figs. B1 and B2 show that the new closed-form expressions are significantly closer to the exact solutions.

7.4. *Expressions for a solute with a retardation factor*

The closed-form expressions applies also to solutes or tracers having a retardation factor R resulting from a partition coefficient k_d between the liquid phase and a solid phase. In equation (6), setting R = 1 and ω' = R·ω, which corresponds to A' = A / R, leaves the equation unchanged. It is then possible to use all the derived expressions, replacing ω by R·ω, to obtain the concentration for a solute with a known retardation factor equal to R. On the other hand, using the original dimensionless expressions to determine the unknown transport parameters ω and α_L from a tracer test, would yield the right value for α_L, but a value of ω multiplied by R. It would then be impossible to determine the value of the retardation factor.

7.5. *Expressions for a solute subject to degradation*

The closed-form expressions may be adapted easily for solutes or tracers subject to an exponential decay during transport as $C_0 e^{-\frac{t}{T_g}}$, *Tg* being the first-order decay time constant for the mobile phase. Assuming the same decay time constant in the solid phase, eq. (6) becomes:

$$R\frac{\partial C}{\partial t} = \alpha_L \frac{A}{r}\frac{\partial^2 C}{\partial r^2} - \varepsilon \frac{A}{r}\frac{\partial C}{\partial r} - R\frac{C}{T_g} \quad (29)$$

Using the dimensionless decay time constant: $T_{gD} = T_g/t_a$, the dimensionless equivalent of eq. (7) is

$$2R\frac{\partial C_D}{\partial t_D} = \frac{1}{P \cdot r_D}\frac{\partial^2 C_D}{\partial r_D^2} - \varepsilon \frac{1}{r_D}\frac{\partial C_D}{\partial r_D} - 2R\frac{C_D}{T_{gD}} \quad (30)$$

It can be verified that if $C_D(r_D, t_D)$ is solution of eq. (7) then $C_D^{'}(r_D, t_D) = C_D(r_D, t_D) \cdot e^{-\frac{t_D}{T_{gD}}}$ is solution of eq. (30)

$$C_D = C_D^{'} \cdot e^{\frac{t_D}{T_{gD}}} \quad (31a)$$

$$\frac{\partial C_D}{\partial t_D} = \frac{\partial C_D^{'}}{\partial t_D} \cdot e^{\frac{t_D}{T_{gD}}} + \frac{C_D^{'}}{T_{gD}} \cdot e^{\frac{t_D}{T_{gD}}} \quad (31b)$$

$$\frac{\partial C_D}{\partial r_D} = \frac{\partial C_D^{'}}{\partial r_D} \cdot e^{\frac{t_D}{T_{gD}}} \quad (31c)$$

$$\frac{\partial^2 C_D}{\partial r_D^2} = \frac{\partial^2 C_D^{'}}{\partial r_D^2} \cdot e^{\frac{t_D}{T_{gD}}} \quad (31d)$$

Introducing eqs. (31a-31d) into eq. (7) and dividing by $e^{\frac{t_D}{T_{gD}}}$ results in eq. (30). This proves that using the new closed-form expressions derived in this paper that are very close to solution of eq. (7), and multiplying

Table 1
Characteristics of the 12 radially convergent tracer tests.

No	Distance to well	Formation thickness	Pumping rate	Duration of test	Name
	m	m	m^3/h	hour	
1	13.9	6.25	39.5	49	Ginger_1
2	15	10	38.5	46	Ginger_2
3	12	8.5	22	24	Ginger_3
4	20	8.5	22	22	Ginger_4
5	20	10.35	24.1	30	Astaillac
6	19.5	10.35	24.1	28.4	Astaillac
7	14.43	8	45	47.3	Tauriac
8	14.04	11	25	48	Bretenoux
9	7.9	11	25	47.9	Bretenoux
10	13	2.5	3.5	177.7	Bonaud INa (09/1977)
11	9	2	4	45.6	Test_4 (Sauty, 1978)
12	200	12	138.6	502	South Farm (Atkinson 2000)
Median	14	9.3	24.6	46.7	

Table 2
Transfer parameters obtained for the 12 tracer tests using the new closed-form expression in unbounded domain.

No	Dispersivity α_L	Kinematic porosity	Péclet number r_L / α_L	Injected mass	Nash coefficient
unit	m	[-]	[-]	g	[-]
1	0.49	0.186	28.2	0.6	0.996
2	6.21	0.036	2.42	191	0.996
3	3.03	0.014	3.96	173	0.945
4	4.30	0.017	4.65	50.4	0.987
5	9.38	0.020	2.13	36.9	0.979
6	7.12	0.012	2.74	38.9	0.972
7	2.47	0.141	5.84	217	0.895
8	3.47	0.063	4.04	222	0.974
9	1.73	0.068	4.57	0.698	0.974
10	1.52	0.078	8.56	137	0.994
11	2.64	0.106	3.41	34.8	0.999
12	32.6	0.014	6.14	144	0.932
Median	3.3	0.049	4.3	93.7	0.977

them by $e^{-\frac{t_D}{T_{gD}}}$ gives approximate closed-form expressions integrating degradation, provided that the boundary conditions are also multiplied by $e^{-\frac{t_D}{T_{gD}}}$. This applies to the slug injections, however for continuous injections it would apply only if the solute is degraded with the same decay rate before being injected, which is usually not verified, as bacterial degradation occurs only in the aquifer.

Fig. 12 refers to the BTCs resulting from a slug injection in converging or diverging flow in an unbounded domain for two Péclet numbers and various decay time constants. It shows that the closed-form expression applies accurately to solutes subject to exponential decay.

It has also been verified that for a bounded domain the equivalent expression applies also with the same accuracy.

8. Application to field tracer tests

The new closed-form expression established in this paper for a slug injection, has been applied for the interpretation of a set of tracer tests, i.e. for determining their dispersivity and kinematic porosity by calibration. It was thus possible to quantify the improvement obtained by using this expression rather than other approximate expressions. The set

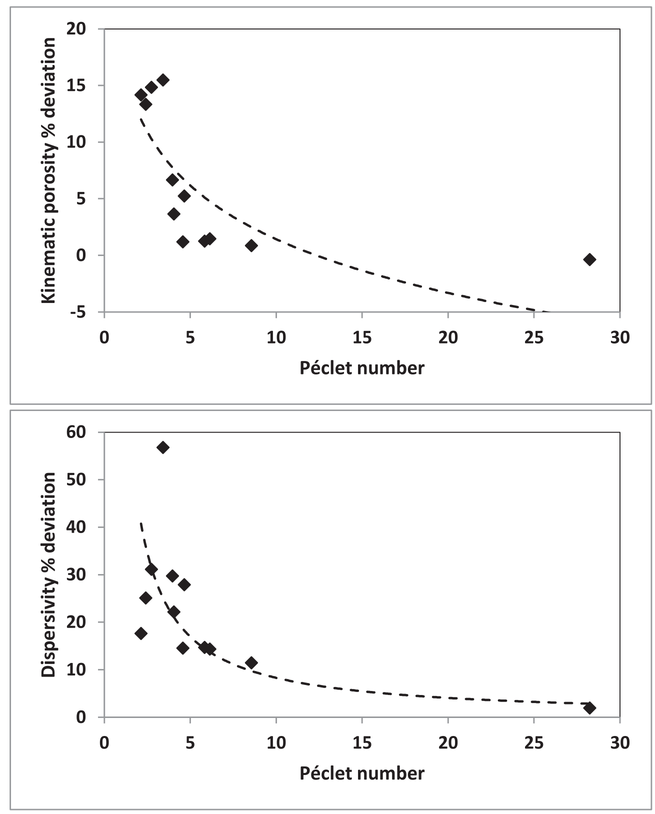

Fig. 13. Twelve field tracer tests: deviations in kinematic porosity (upper part) and dispersivity (lower part) using the formulation of Wang & Crampon (1995) compared to using the new quasi exact closed form approximation in unbounded domain.

Table 3
Transfer parameters obtained for the 12 tracer tests using the expression of Wang & Crampon (1995), and deviations from the new closed-form expression in unbounded domain.

No	Dispersivity α_L	Dispersivity α_L	Kinematic porosity	Kinematic porosity	Péclet number (reference)
	m	% deviation	[-]	% deviation	[-]
1	0.50	1.9	0.185	−0.4	28.2
2	7.77	25	0.041	13	2.4
3	3.93	30	0.015	6.7	4.0
4	5.50	28	0.017	5.2	4.7
5	11.0	18	0.023	14	2.1
6	9.33	31	0.013	15	2.7
7	2.83	15	0.142	1.3	5.8
8	4.24	22	0.065	3.7	4.0
9	1.98	15	0.069	1.2	4.6
10	1.69	12	0.079	0.9	8.6
11	4.13	57	0.123	15	3.4
12	37.3	14	0.014	1.5	6.1
Median	4.2	19.9	0.053	4.4	4.3

consists of twelve tracer tests, mostly performed in alluvial formations. Tracer tests #1 through #8 come from Gutierrez et al. (2012). The BTCs data relative to these tracer tests are provided as "Supplementary material". The main characteristics of the tests (distance to well, formation thickness, pumping rate, test duration) are gathered in Table 1. The distance from the injection point to the pumping well is most of the time quite small (median value is 14 m) with only one exception. The formations thickness are also small (median thickness is 9.3 m) and the total duration of the tests usually ranges from 1 day to 2 days, with the exception of two much longer tests. Unfortunately the injected masses were not known.

Using the Rosenbrock optimization method for determining the optimal kinematic porosity and dispersivity, the BTCs of these twelve tracer tests were reproduced successfully with the new closed-form formulation in unbounded domain, eq. (21, 22a, 22b). The median Nash and Sutcliffe criterion is 0.977 with only one value below 0.9. The calibrated kinetic porosity, dispersivity and injected mass values are given in Table 2. The Péclet numbers obtained are rather small (median value is 4.3) and only one value is above 10.

Two approximate expressions for a slug injection in converging flow were used for comparison: the expressions described by Sauty (1980) and by Wang and Crampon (1995).

Sauty's (1980) expression is eq. (26), the derivative versus time of Ogata and Banks (1961) equation for a step injection in 1D Cartesian coordinate (Lenda and Zuber, 1970), without correction factors. The Wang and Crampon (1995) equation for a radially convergent slug injection, for the whole BTC, is based on eq. (19), i.e. the solution of a slug injection in 1D Cartesian coordinate with correction factors. It is valid only for Péclet numbers greater than 3:

$$C_D(t_D) = K\sqrt{\frac{P/f_P}{4\pi t_D/f_T}}\cdot\exp\left[-\frac{P/f_P}{4t_D/f_T}(1-t_D/f_T)^2\right]$$

with

K = Normalization constant

$$f_T = 2\cdot(0.503 - 0.33/P) \text{ if } P\leqslant 100; \quad \text{else } f_T = 1$$

$$f_P = 1.32 - 1.116/P$$

The twelve BTCs were also reproduced successfully using both these approximate expressions, with comparable Nash coefficients. However the calibrated values of the kinetic porosity and of the dispersivity, given in Table 3 for the Wang and Crampon (1995) equation, differ significantly from those obtained using the new closed-form expression of this paper, which is extremely close to the exact solution. Using the formulation of Wang and Crampon (1995), both of these parameters are overestimated. The median value of the overestimation is 19.9% for dispersivity and only 4.4% for kinematic porosity. Fig. 13 shows that, as expected, it is for small Péclet numbers that the new closed-form expression provides more accuracy, where the overestimation of the dispersivity was the largest.

Sauty's (1980) approximation heavily overestimates the dispersivity and kinematic porosity. The median value of these two parameters overestimation is 69% and 67% respectively. However Sauty's (1980) approximate formulation was selected after comparison to a numerical modeling using an outer boundary condition not clearly documented, but apparently corresponding to a bounded domain. Therefore another comparison was made with the kinematic porosity and dispersivity obtained with the new closed-form expression of this paper in a bounded domain, eq. (27, 28a, 28b). The deviations are then smaller: the median value of the overestimation is reduced to 15.4% for dispersivity, and to 23.2% for kinematic porosity.

9. Summary and conclusions

This paper derived simple accurate approximate closed-form expressions for tracer injection in aquifer with a radially converging or diverging flow in a bounded or unbounded domain. Starting from approximate closed-form expressions for a slug injection or a continuous injection in 1D Cartesian coordinate, two correction coefficients, depending only on the Péclet number, were introduced into this expression to obtain new closed-form expressions that most accurately reproduce the exact solutions in radial coordinate. The conditions of application of these expressions are that the aquifer must have homogeneous properties and a uniform thickness, and the central pumping (or injection) well must have a negligible radius. Longitudinal dispersion is taken into account, but the molecular diffusion is neglected. Transverse dispersion does not appear in the expressions because it has no influence. The closed-form expressions may be used for a tracer having a retardation factor and subject to exponential degradation.

An interesting result, obtained by the numerical simulations, is that for a given set of parameters, a BTC at the sampling well is identical in diverging or in converging flow. This applies in unbounded domain and also in bounded domain.

Using the 4 following dimensionless numbers:

$t_D = t\cdot Q/(\pi r_L^2 h\omega)$ Dimensionless time,

$P = r_L/\alpha_L$ Péclet number,

$C_D = C\cdot Q/q_m$ Dimensionless concentration for a continuous injection, or

$C_D = C\cdot\pi r_L^2 h\omega/M$ Dimensionless concentration for a slug injection,

the approximate closed-form, for Péclet number ranging from 1 to 1000, and dimensionless time ranging from 0 to 5, are:

Unbounded domain

Slug injection:

$$C_D(t_D) = 0.5\cdot f_T\sqrt{\frac{P/f_P}{4\pi f_T.t_D}}\cdot\frac{(f_T\cdot t_D+1)}{f_T.t_D}\cdot\exp\left[-\frac{P/f_P}{4f_T\cdot t_D}(1-f_T\cdot t_D)^2\right]\cdot e^{-\frac{t_D}{T_{gD}}}$$

$$f_T = 1.00092 - 0.45272\cdot P^{-0.87334}$$

$$f_P = 1.51016 - 0.3189\cdot P^{-0.09496}$$

(When there is no degradation, $T_{gD} = \infty$ and the last term is dropped.)

Continuous injection:

$$C_D = 0.5\cdot\text{erfc}\left[\sqrt{\frac{P/f_P}{4f_T\cdot t_D}}(1-f_T\cdot t_D)\right]$$

$$f_T = 1.00627 - 0.44829\cdot P^{-0.73712}$$

$$f_P = 1.44488 - 0.21574\cdot P^{-0.78005}$$

Bounded domain

These expressions in a bounded domain can be used for tracer tests in converging flow, they would not be appropriate in diverging flow.

Slug injection:

$$C_D(t_D) = f_T\sqrt{\frac{P/f_P}{4\pi f_T.t_D}}\cdot\exp\left[-\frac{P/f_P}{4f_T\cdot t_D}(1-f_T\cdot t_D)^2\right]\cdot e^{-\frac{t_D}{T_{gD}}}$$

$$f_T = 0.99003 + 1.29039\cdot P^{-0.72566}$$

$$f_P = 1.51514 - 0.89053\cdot P^{-0.29830}$$

Continuous injection:

$$C_D(t_D) = 0.5\left\{\mathrm{erfc}\left[\sqrt{\frac{P/f_P}{4f_T\cdot t_D}}(1 - f_T\cdot t_D)\right] + \exp(P/f_P)\cdot\mathrm{erfc}\left[\sqrt{\frac{P/f_P}{4f_T\cdot t_D}}(1 + f_T\cdot t_D)\right]\right\}$$

$$f_T = 1.17097 - 0.20663\cdot P^{-1.87515}$$

$$f_P = 1.43094 - 0.96565\cdot P^{-0.47269}$$

The new closed-form formulation for a slug injection in unbounded domain has been applied to twelve radially convergent tracer tests. The mass transfer parameters obtained were compared to those obtained by two approximate methods: Sauty's (1980) formulation and the formulation of Wang and Crampon (1995). It appeared that Sauty's (1980) approximate formulation results in overestimations of both the kinematic porosity and the dispersivity. Using the approximate formulation of Wang and Crampon (1995) also overestimates dispersivity, but to a lesser extent.

It has been shown that by choosing a bounded domain, to reduce the spurious upstream dispersion, instead of an unbounded domain corresponding to the real geometry, significantly different values are obtained for the dispersivity, but also for the porosity. These differences however decrease for large Péclet numbers. It has also been shown that both schemes can reproduce the BTC equally well; therefore, the analysis of the BTC alone does not allow the selection of the most appropriate scheme.

Funding information

This research was conducted by the French Geological Survey (BRGM), and was funded by internal research projects.

Declaration of Competing Interest

The authors declare that they have no known competing financial interests or personal relationships that could have appeared to influence the work reported in this paper.

Acknowledgements

The authors are grateful to T. Klinka from BRGM for providing field tracer tests data to apply the developed solutions. They are also grateful to the two anonymous reviewers for their helpful suggestions.

Appendix. A. Validation of our 1D radial numerical scheme, discretization and outer boundary conditions in bounded domain

Our 1D radial numerical scheme and discretization was validated in bounded domain in converging flow by comparison to Chen et al. (2002) analytical solution as depicted in their Fig. 2 and Fig. 4. Fig. A1 and Fig. A2 show that the numerical calculations, with the selected spatial and temporal discretization and outer boundary condition reproduce accurately the exact analytical solution of Chen et al. (2002) for Péclet numbers ranging from 0.1 to 200.

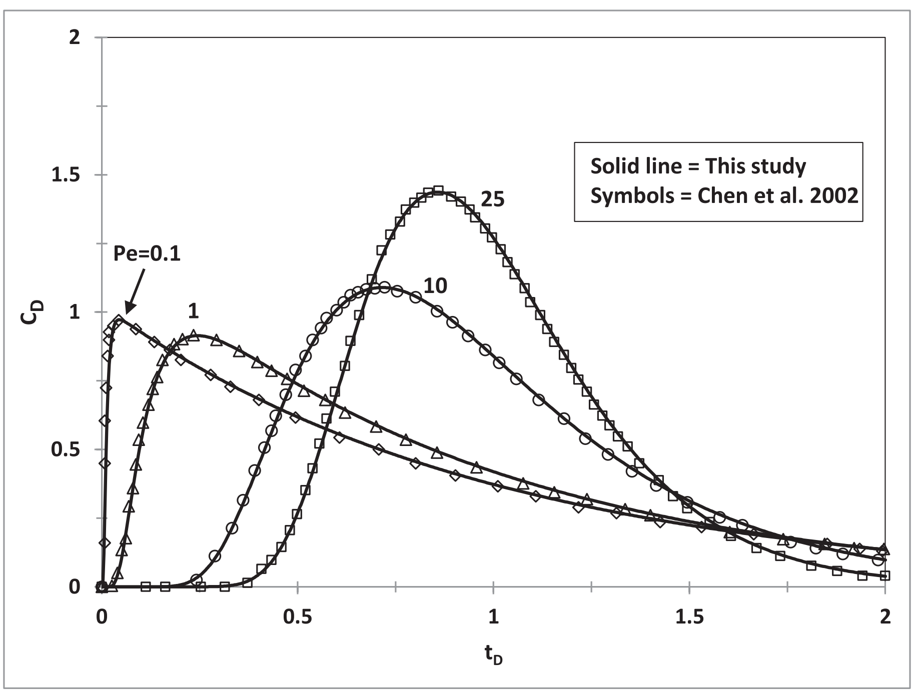

Fig. A1. Dimensionless BTCs in a bounded domain in a converging flow obtained with the numerical model [solid line], compared with the solution of Chen et al. (2002) [symbols]. Péclet numbers from 0.1 to 25.

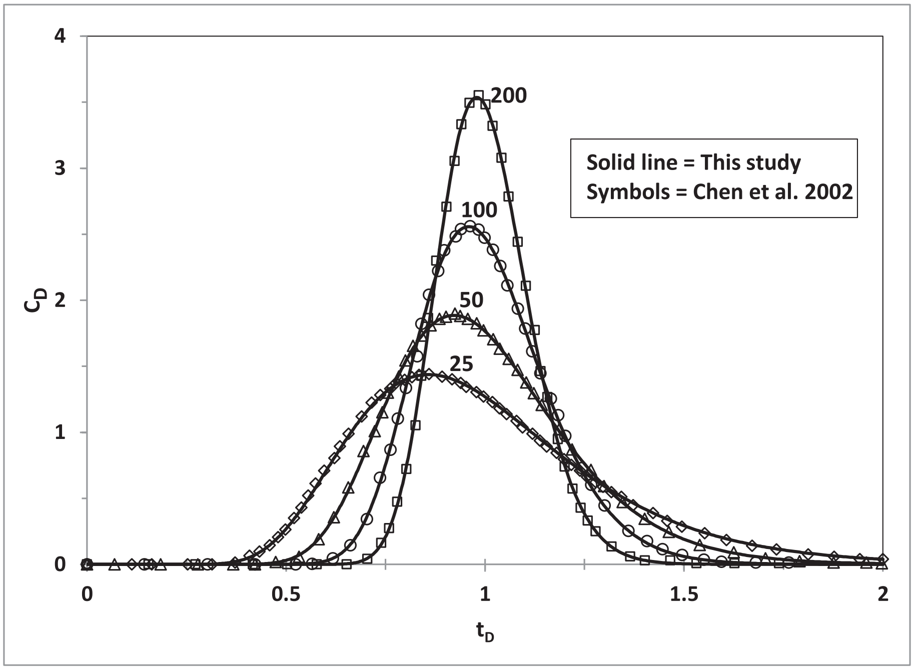

Fig. A2. Dimensionless BTCs in a bounded domain in a converging flow obtained with the numerical model [solid line], compared with the solution of Chen et al. (2002) [symbols]. Péclet numbers from 25 to 200.

Appendix B. . Evaluating the improvement of the new closed-form expressions

The improvement of the new closed-form expressions developed in this paper is demonstrated by comparison to the two approximate closed-form available for the BTC resulting from a slug injection in radial flow: Sauty's (1980) closed-form for a slug injection in converging flow, and the closed-form described by Wang and Crampon (1995) for the whole BTC duration. The equations corresponding to these approximate expressions are given in Section 8.

Sauty's (1980) approximation for a slug injection in converging flow

In the numerical model used by Sauty (1980) to select its approximate expression, the outer boundary condition although not clearly documented corresponds apparently to a bounded domain. For this reason their approximation was compared to the solution in a bounded domain and the closeness to their solution was compared the new closed-form in a bounded domain.

Fig. B1 shows that the new closed-form expression in bounded domain, eq. (27, 28a, 28b), is significantly closer to the exact solution than Sauty's (1980) expression. This is true as well for small Péclet numbers not exceeding 3 as for large values exceeding 30.

Wang and Crampon (1995) approximation

Wang and Crampon (1995) used a numerical model in unbounded domain to fit their expressions. Among the four expressions, ascending part of BTC or whole BTC, converging or diverging, only the two expressions for the whole BTC were selected and compared to the single exact solution. The closeness of their expressions, valid for Péclet number greater than or equal to 3, were compared to the single new closed-form in unbounded domain.

In unbounded domain also, Fig. B2 shows that the new closed-form expression, eq. (21, 22a, 22b), is much closer to the exact solution than Wang and Crampon (1995) expression. The difference is considerable for small Péclet numbers not exceeding 3, which are below the limit of validity of their expression, but is also significant for larger values. The difference decreases, however, for large values exceeding 30.

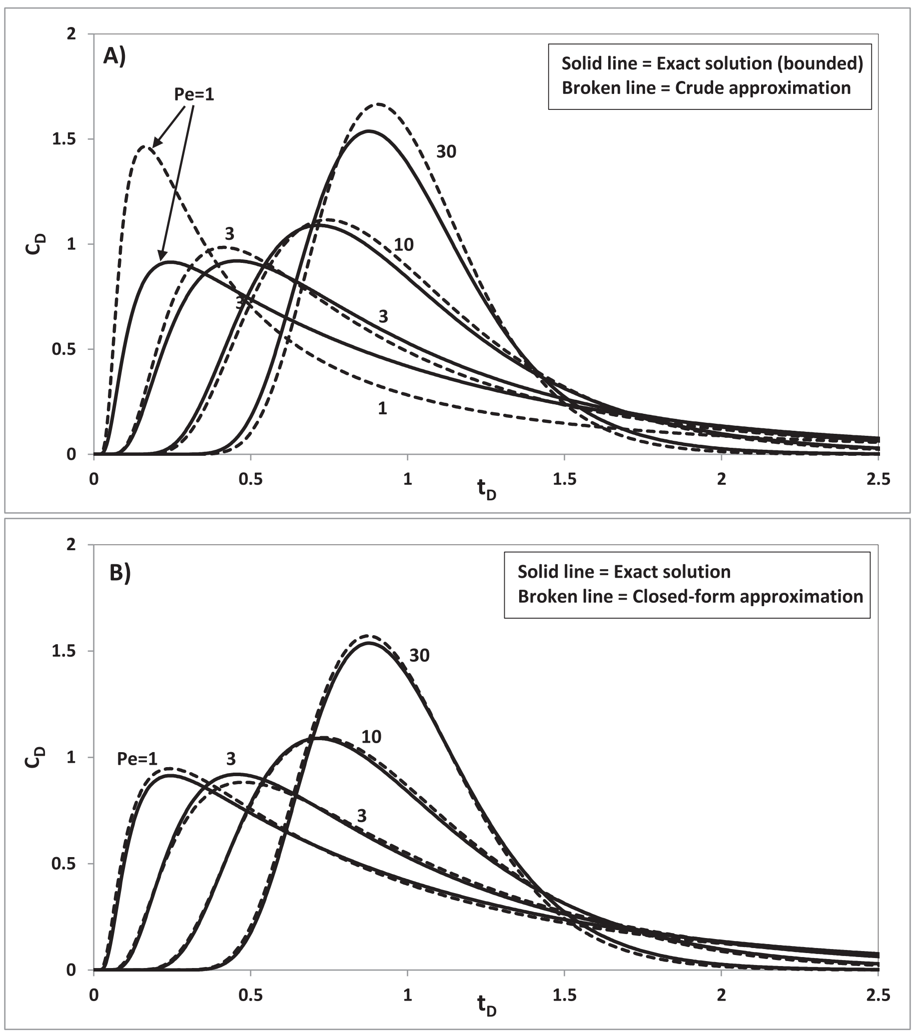

Fig. B1. Exact solution of BTCs in radial bounded domain compared to: A) Sauty's (1980) approximate solution; B) This paper new closed-form approximation.

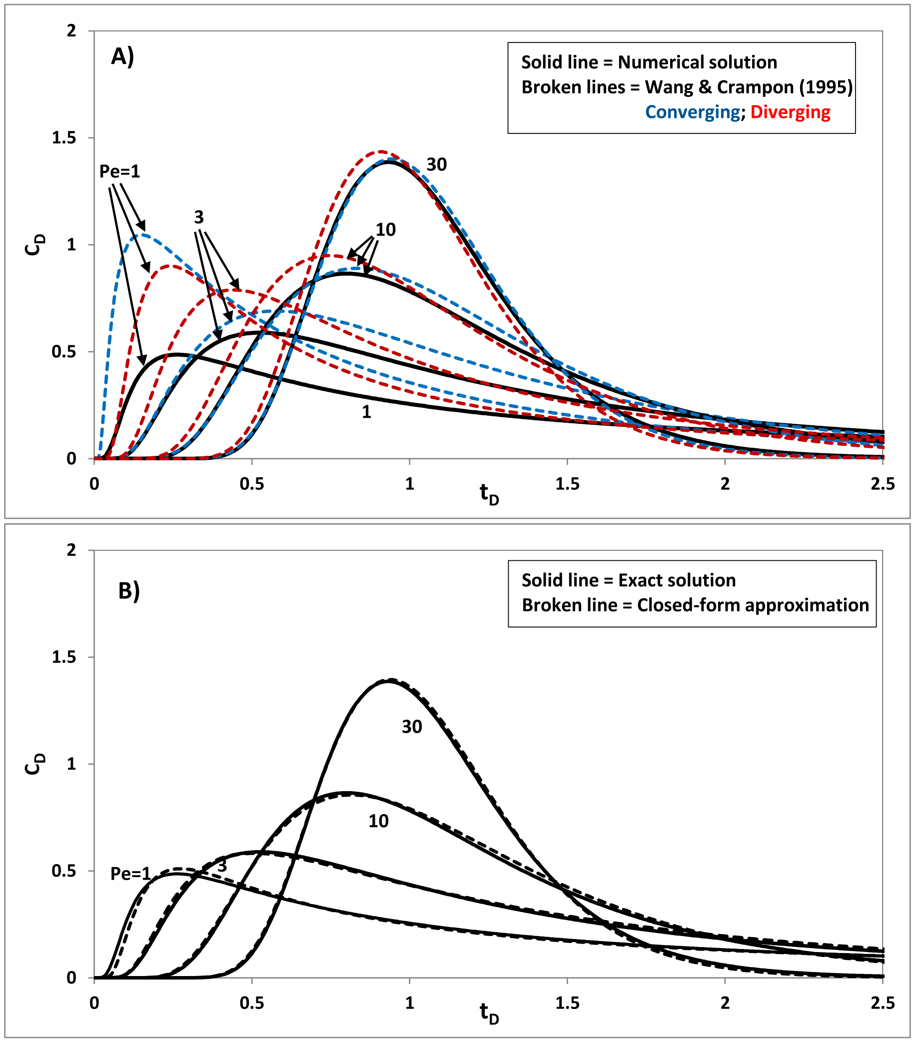

Fig. B2. Exact solution of BTCs in radial unbounded domain compared to: A) the approximate solution of Wang and Crampon (1995); B) this paper new closed-form approximation.

Appendix C. . Comparison of the transport parameters obtained in a tracer test analysis using expressions for a bounded or unbounded domain

The transport parameters, kinematic porosity and dispersivity, obtained from the analysis of a tracer test, depend on the assumption chosen for the domain: bounded or unbounded.

To analyze the sensitivity to this assumption, the dimensionless BTCs for slug injections were calculated with the exact bounded domain solution for 20 values of Péclet numbers, corresponding to given values of kinematic porosity and dispersivity.

These 20 BTCs are assumed to represent actual tracer tests. Using the exact solution corresponding to the alternative assumption of an unbounded domain, the 20 BTCs are analyzed to determine the corresponding kinematic porosity and dispersivity. It can be seen from Fig. C1 that all BTCs corresponding to Péclet numbers greater than or equal to 1.5 could be reproduced very accurately with the unbounded domain solution, but with transport parameters different from the original parameters. This shows that the sole analysis of a BTC cannot help to determine which geometry, bounded or not, should be selected. Fig. C2 shows the changes in the initial parameters required to reproduce the BTCs. It appears that in the unbounded domain, the corresponding calibrated dispersivity is decreased by 50%, 20%, and 8% respectively for Péclet numbers equal to 1.5, 10 and 30. The corresponding calibrated kinematic porosity is decreased by 38%, 15% and 7% for these same Péclet numbers. The reason for the decrease in dispersivity is that without upstream dispersion, the BTCs are less dispersed, especially for small Péclet numbers. The decrease in kinematic porosity is also explained by the fact that without upstream dispersion, the bulk advection velocity is increased, resulting in a decrease in porosity.

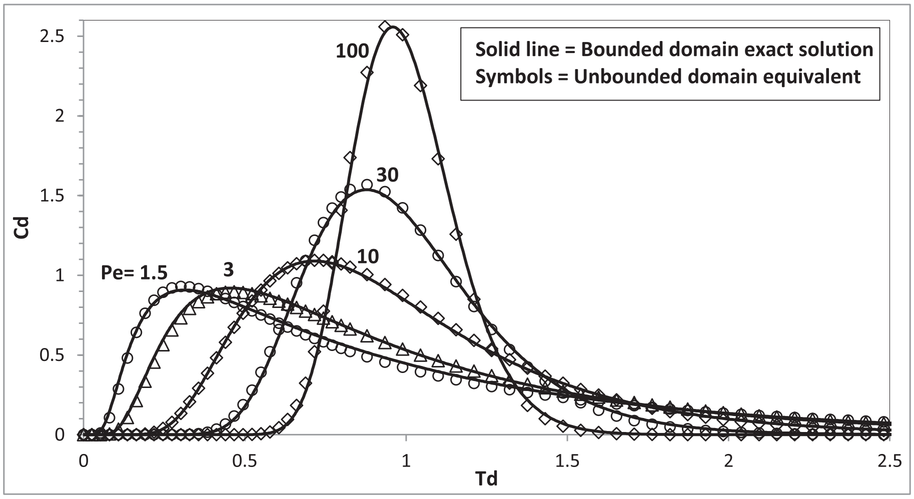

Fig. C1. Exact solution in bounded domain: calibration in unbounded domain with modified parameters.

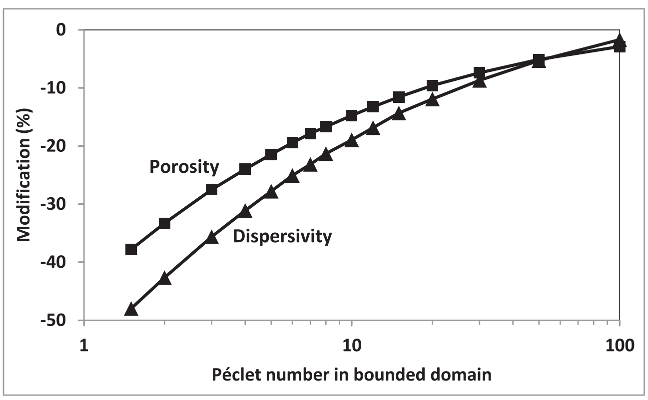

Fig. C2. Exact solution in bounded domain: modification of the porosity and dispersivity resulting from a calibration in unbounded domain.

Appendix D. Supplementary data

Supplementary data to this article can be found online at https://doi.org/10.1016/j.jhydrol.2022.127661.

References

Akanji, L.T., Falade, G.K., 2018. 2018 - Closed-Form Solution of Radial Transport of Tracers in Porous Media Influenced by Linear Drift. Energies 12 (1), 29. https://doi.org/10.3390/en12010029.

Bear, J., 1972. Dynamics of Fluids in Porous Media. Elsevier, New York.

Becker, M.W., Charbeneau, R.J., 2000. Erratum: first-passage-time transfer functions for groundwater tracer tests conducted in radially convergent flow. J. Contam. Hydrol. 45, 361–372.

Chen, J.S., Liu, C.W., Chen, C.S., Yeh, H.D., 1996. A Laplace transform solution for tracer test in a radially convergent flow with upstream dispersion. J. Hydrol. 183, 263–275.

Chen, J.-S., Liu, C.-W., Liao, C.-M., 2002. A novel analytical power series solution for solute transport in a radially convergent flow field. J. Hydrol. 266 (1-2), 120–138.

Chen, J.-S., Liu, C.-W., Chen, C.-S., Liao, C.-M., 2003a. Effect of well bore mixing volume on non-axisymmetrical transport in a convergent radial tracer test. J. Hydrol. 277 (1), 61–73. https://doi.org/10.1016/S0022-1694(03)00082-9.

Chen, J.-S., Liu, C.-W., Hsu, H.-T., Liao, C.-M., 2003b. A Laplace transform power series solution for solute transport in a convergent flow field with scale-dependent dispersion. Water Resour. Res. 39 (8), 1229. https://doi.org/10.1029/2003WR002299.

Csanady, G.T., 1973. Turbulent Diffusion in the Environment. D. Reidel Publishing Company, Dordrecht, Holland. DOI:10.1007/978-94-010-2527-0.

Field, M., 2002. The QTRACER2 program for tracer-breakthrough curve analysis for tracer tests in karstic aquifers and other hydrologic systems; EPA/600/R-02/001.

Gutierrez, A., Klinka, T., Thiéry, D., Buscarlet, E., Binet, S., et al. 2013. TRAC, a collaborative computer tool for tracer-test interpretation. 6th International Conference on Tracers and Tracing Methods, Jun 2011, Oslo, Norway. 8 p., EPJ Web of Conferences 50, 03002 (2013) doi.org/10.1051/epjconf/20135003002.

Gutierrez, A., Klinka, T., Thiéry, D., 2012 - Manuel d'utilisation de TRAC : Aide à l'interprétation de traçages en milieux poreux. BRGM report RP-60660-FR (*in French*). http://infoterre.brgm.fr/rapports/RP-60660-FR.pdf.

Irvine, D.J., Werner, A.D., Ye, Y., A. Jazayeri, A., 2020 - Upstream Dispersion in Solute Transport Models: A Simple Evaluation and Reduction Methodology. Groundwater J. 59(2). doi.org/10.1111/gwat.13036.

Käss, W., 1998. Tracing Technique in Geohydrology; A. A. Balkema, Rotterdam, Brookfield, Vt., 581 p.

Lenda, A., Zuber, A., 1970. Tracer dispersion in groundwater experiments. In: Isotope Hydrology. International Atomic Energy Agency, Vienna, pp. 619–641.

Leonard, B.P., 1988. Universal Limiter for transient interpolation modeling of the advective transport equations: the ULTIMATE conservative difference scheme, NASA Technical Memorandum 100916 ICOMP-88-11.

Moench, A.F., 1989. Convergent radial dispersion: a Laplace transform solution for aquifer tracer testing. Water Resour. Res. 25 (3), 439–447.

Moench, A.F., 1995. Convergent radial dispersion in a double-porosity aquifer with fracture skin: analytical solution and application to a field experiment in fractured chalk. Water Resour. Res. 31 (8), 1823–1835.

Nash, J.E., Sutcliffe, J.V., 1970. River flow forecasting through conceptual models part I — A discussion of principles. J. Hydrol. 10 (3), 282–290. https://doi.org/10.1016/0022-1694(70)90255-6.

Natarajan, N., 2016. Effect of distance-dependent and time-dependent dispersion on non-linearly sorbed multispecies contaminants in porous media. ISH J. Hydraul. Eng. 22 (1), 16–29. https://doi.org/10.1080/09715010.2015.1043597.

Ogata, A., 1958. Dispersion in porous media, Ph.D. thesis. Northwestern Univ, Evanston, Ill.

Ogata, A. et Banks, R.B., 1961. A solution of the differential equation of longitudinal dispersion in porous media. U.S. Geol. Surv., Prof. Pap. 411-A.

Pérez Guerrero, J.S., Skaggs, T.H., 2010. Analytical solution for one-dimensional advection-dispersion transport equation with distance-dependent coefficients. J. Hydrol. 390 (1–2), 57–65. https://doi.org/10.1016/j.jhydrol.2010.06.030.

Rosenbrock, H.H., 1960. An automatic method for finding the greatest or the least value of a function; Computer journal 3.3., p. 175-184, Oct. 1960.

Sauty, J.-P., 1977a. Contribution à l'identification des paramètres de dispersion dans les aquifères par l'interprétation des expériences de traçage, D.Ing. Thesis, Univ. Sci. et Méd. de Grenoble, France (*in French*).

Sauty, J.-P., 1978. Identification des paramètres du transport hydrodispersif dans les aquifères par interprétation de traçages en écoulement cylindrique convergent ou divergent. J. Hydrol. 39 (1–2), 69–103. https://doi.org/10.1016/0022-1694(78)90115-4.

Sauty, J.-P., 1980. An analysis of hydrodispersive transfer in aquifers. Water Resour. Res. 16 (1), 145–158.

Thiéry, D., 2010. Groundwater Flow Modeling in Porous Media Using MARTHE. *in "Modeling Software Volume 5, Chapter 4, pp. 45-60 • Environmental Hydraulics Series"*. Tanguy J.M. (Ed.) – Wiley Editions/ISTE London. ISBN: 978-1-84821-157-5.

Thiéry, D., 2015b. Modélisation 3D du transport de masse et du transfert thermique avec le code de calcul MARTHE – version 7.5. Rapport BRGM/RP-64765-FR, 324 p., 158 fig. (*in French*). http://infoterre.brgm.fr/rapports/RP-64765-FR.pdf.

Thiéry, D. and Picot-Colbeaux, G., 2020 – Guidelines for MARTHE v7.8 computer code for hydro-systems modelling (English version). Report BRGM/RP-69660-FR, 246 p., 177 fig. http://infoterre.brgm.fr/rapports//RP-69660-FR.pdf.

Toride, N., Leij, F.J., Van Genuchten, M.Th., 1999. The CXTFIT code for estimating transport parameters from laboratory or field tracer experiments. Version 2.1, Research Report n°137, U.S. Salinity Lab., Riverside, CA.

Vanderborght, J., Kasteel, J., Herbst, M., Javaux, M., Thiéry, D., Vanclooster, M., Mouvet, C., Vereecken, H., 2005. 2005 - A set of Numerical Models for Simulating Flow and Transport in Soils Using Analytical Solutions. Vadose Zone J 4 (1), 206–221. https://doi.org/10.2136/vzj2005.0206.

Van Genuchten, M.T., 1985. Convective-dispersive transport of solutes involved in sequential first-order decay reactions. Comput. Geosci. 11 (2), 129–147.

Van Genuchten, M.T., 1981. Analytical solutions for chemical transport with simultaneous adsorption, zero-order production and first order decay. J. Hydrol. 49 (3-4), 213–233. https://doi.org/10.1016/0022-1694(81)90214-6.

Wang, H.Q., Crampon, N., 1995. Method for interpreting tracer experiments in radial flow using modified analytical solutions. J. Hydrol. 165 (1–4), 11–31. https://doi.org/10.1016/0022-1694(94)02588-3.

Wang, Q., Zhan, H., 2013. Radial reactive solute transport in an aquifer–aquitard system. Adv. Water Resour. 61 (2013), 51–61. https://doi.org/10.1016/j.advwatres.2013.08.013.

Welty, C., Gelhar, L.W., 1994. Evaluation of longitudinal dispersivity from nonuniform flow tracer tests. J. Hydrol. 153 (1-4), 71–102. https://doi.org/10.1016/0022-1694(94)90187-2.

Zlotnik, V.A., Logan, J.D., 1996. Boundary conditions for convergent radial tracer tests and the effect of well bore mixing volume. Water Resour. Res. 32 (7), 2323–2328.